

DOE/PC/92528--9

CHAR PARTICLE FRAGMENTATION AND ITS EFFECT ON  
UNBURNED CARBON DURING PULVERIZED COAL  
COMBUSTION

Quarterly Report for the Period

October 1, 1994 - December 31, 1994

Grant DE-FG22-92PC92528

Prepared for

THE UNITED STATES DEPARTMENT OF ENERGY

James Hickerson  
Project Officer  
Pittsburgh Energy Technology Center  
Pittsburgh, PA 15236

Submitted by

Professor Reginald E. Mitchell

March 1995

08 DISTRIBUTION OF THIS DOCUMENT IS UNLIMITED

HIGH TEMPERATURE GASDYNAMICS LABORATORY  
Mechanical Engineering Department  
Stanford University

MASTER

RECEIVED  
USDOE/PETC  
05 MAR 31 AM 10:32  
ASSISTANCE DIV.

L  
G  
T  
H

U. S. DEPARTMENT OF ENERGY

UNIVERSITY CONTRACTOR, GRANTEE, AND COOPERATIVE AGREEMENT  
RECOMMENDATIONS FOR ANNOUNCEMENT AND DISTRIBUTION OF DOCUMENTS

See Instructions on Reverse Side

1. DOE Report No.

3. Title  
Char Particle Fragmentation and its Effects on  
Unburned Carbon During Pulverized Coal Combustion

2. DOE Contract No.  
DE-FG22-92PC92528 -9

4. Type of Document ("x" one)

- a. Scientific and technical report
- b. Conference paper:

Title of conference \_\_\_\_\_

Date of conference \_\_\_\_\_

Exact location of conference \_\_\_\_\_

Sponsoring organization \_\_\_\_\_

c. Other (Specify) R&D Report

5. Recommended Announcement and Distribution ("x" one)

- a. Unrestricted unlimited distribution.
- b. Make available only within DOE and to DOE contractors and other U. S. Government agencies and their contractors.
- c. Other (Specify) \_\_\_\_\_

6. Reason for Recommended Restrictions

7. Patent and Copyright Information:

- Does this information product disclose any new equipment, process, or material?  No  Yes If so, identify page nos. \_\_\_\_\_
- Has an invention disclosure been submitted to DOE covering any aspect of this information product?  No  Yes
- If so, identify the DOE (or other) disclosure number and to whom the disclosure was submitted.
- Are there any patent-related objections to the release of this information product?  No  Yes If so, state these objections.
- Does this information product contain copyrighted material?  No  Yes
- If so, identify the page numbers \_\_\_\_\_ and attach the license or other authority for the government to reproduce.

8. Submitted by

Name and Position (Please print or type)

Reginald E. Mitchell, Associate Professor

Organization

Stanford University

Signature

*Reginald E. Mitchell*

Phone

(415) 723-1745

Date

3/25/95

FOR DOE OR OTHER AUTHORIZED  
USE ONLY

9. Patent Clearance ("x" one)

- a. DOE patent clearance has been granted by responsible DOE patent group.
- b. Report has been sent to responsible DOE patent group for clearance.

## **DISCLAIMER**

**Portions of this document may be illegible in electronic image products. Images are produced from the best available original document.**

# CHAR PARTICLE FRAGMENTATION AND ITS EFFECT ON UNBURNED CARBON DURING PULVERIZED COAL COMBUSTION

Quarterly Report for the Period

October 1, 1994 - December 31, 1994

Grant DE-FG22-92PC92528

Prepared for

THE UNITED STATES DEPARTMENT OF ENERGY

James Hickerson  
Project Officer  
Pittsburgh Energy Technology Center  
Pittsburgh, PA 15236

Submitted by

Professor Reginald E. Mitchell

This report was prepared as an account of work sponsored by the United States Government. Neither the United States nor the United States Department of Energy, nor any of their employees, makes any warranty, expressed or implied, or assumes any legal liability or responsibility for the accuracy, completeness, or usefulness of any information, apparatus, product or process disclosed, or represents that its use would not infringe privately owned rights. Reference herein to any specific commercial product, process, or service by trade name, mark, manufacturer, or otherwise, does not necessarily constitute or imply its endorsement, recommendation, or favoring by the United States Government or any agency thereof. The views and opinions of authors expressed herein do not necessarily state or reflect those of the United States Government or any agency thereof.

March 1995

High Temperature Gasdynamics Laboratory  
Department of Mechanical Engineering  
Stanford University

 DISTRIBUTION OF THIS DOCUMENT IS UNLIMITED

US/DOE Patent Clearance is not required prior to the publication of this document.

**PROJECT TITLE:** CHAR PARTICLE FRAGMENTATION AND ITS EFFECT ON UNBURNED CARBON DURING PULVERIZED COAL COMBUSTION

**ORGANIZATION:** High Temperature Gasdynamics Laboratory  
Stanford University

**CONTRACT:** DOE DE-FG22-92PC92528

**REPORTING PERIOD:** October 1, 1994 - December 31, 1994

**REPORTED BY:** Reginald E. Mitchell

Phone: 415-725-2015

### **RESEARCH OBJECTIVES**

This document is the ninth quarterly status report of work on a project concerned with the fragmentation of char particles during pulverized coal combustion that is being conducted at the High Temperature Gasdynamics Laboratory at Stanford University, Stanford, California. The project is intended to satisfy, in part, PETC's research efforts to understand the chemical and physical processes that govern coal combustion. The work is pertinent to the char oxidation phase of coal combustion and focuses on how the fragmentation of coal char particles affects overall mass loss rates and how char fragmentation phenomena influence coal conversion efficiency. The knowledge and information obtained will allow the development of engineering models that can be used to predict accurately char particle temperatures and total mass loss rates during pulverized coal combustion. In particular, the work will provide insight into causes of unburned carbon in the ash of coal-fired utility boilers and furnaces. Work is to be performed over the three-year period from September 1992 to September 1995.

The proposed study has relevance to char particle fragmentation and its effect on mass loss rates during pulverized coal combustion. Depending on coal type, a significant number of char particles are formed during devolatilization that are categorized as being cenospheres or mesospheres -- particles that have relatively large void volumes within them. Large voids at the outer surfaces of particles allow oxygen to consume the inner particle material. As a consequence, particles may fragment. Fragments burn at rates governed by their individual sizes and not at rates determined by the sizes of their parent char particles. Thus, the overall mass loss rates of char particles that fragment extensively can not be predicted accurately

without accounting for the effects of fragmentation. In this study, to eliminate the complications associated with the complex composition of coals, combustion tests are performed using synthetic chars having particle morphologies similar to those of the char particles formed during coal devolatilization. Results with the synthetic chars are used to define parameters that appear in the char oxidation-fragmentation model being developed. The model is validated by comparing predicted mass loss and fragmentation rates with those measured during combustion tests with real coal chars.

The overall objectives of the project are: (i) to characterize fragmentation events as a function of combustion environment, (ii) to characterize fragmentation with respect to particle porosity and mineral loadings, (iii) to assess overall mass loss rates with respect to particle fragmentation, and (iv) to quantify the impact of fragmentation on unburned carbon in ash. The knowledge obtained during the course of this project will be used to predict accurately the overall mass loss rates of coals based on the mineral content and porosity of their chars. The work will provide a means of assessing reasons for unburned carbon in the ash of coal fired boilers and furnaces.

The project is divided into four research tasks. Specific objectives associated with each task are as follows:

### **Task 1: Production and Characterization of Synthetic Chars**

*Objective:* The objective of this task is to produce and characterize synthetic chars with controlled macroporosity and known mineral content. Densities, porosities, pore size distributions, and total surface areas will be measured. Chemical analyses will be performed to determine the composition of chars that have been laden with pyrites, calcites, silica, and gypsum.

*Deliverables:* Results of this task will yield well-characterized materials for use in combustion and fragmentation studies associated with Tasks 2 and 3 of this project. Particles in the size ranges 75 - 90  $\mu\text{m}$ , 90 - 106  $\mu\text{m}$ , and 106 - 125  $\mu\text{m}$  that have porosities exceeding 60% will be produced.

### **Task 2: Baseline Char Combustion Experiments**

*Objectives:* The objectives of this task are to design and fabricate an entrained flow reactor and a solids extraction probe and to determine gaseous conditions for diffusion-limited combustion of the synthetic chars. The extent to which particles fragment during the extraction process will be characterized.

An additional objective is to employ thermogravimetric analysis to determine the extent to which the overall particle burning rates of the mineral-laden synthetic chars are catalyzed in the gaseous environments that will be used in the fragmentation studies.

***Deliverables:*** The following will result after completion of this task:

- An entrained flow reactor capable of simulating environments typical of pulverized coal combustors and a solids extraction probe that permits sampling of partially reacted chars at different residence times in the reactor.
- Characterization of the extent to which particles fragment during the extraction process.
- Oxygen concentrations and gas temperatures that yield diffusion-limited burning of the synthetic chars produced.
- Characterization of the extent of catalysis in the gaseous environments employed due to mineral constituents of the synthetic chars.

### **Task 3: Char Fragmentation Studies**

***Objective:*** The overall objective of this task is to obtain the data necessary to understand how the porosity of char particles affects their fragmentation behavior and how the minerals in char particles influence their fragmentation patterns.

***Deliverables:*** The following will result after completion of this task:

- A measure of fragmentation events that result as a consequence of burning at diffusion-limited rates in various gaseous environments as a function of particle porosity.
- A measure of how the type of mineral and the mineral content of char affects its fragmentation patterns.

### **Task 4: Fragmentation Modeling**

***Objective:*** The objective of this task is to develop and validate a fragmentation model that can be incorporated into a char oxidation model.

***Deliverable:*** The successful completion of this task will yield a char oxidation-fragmentation model that describes the results of Task 3 experiments. The model will

be capable of accurately predicting overall char mass loss and significant fragmentation events in gaseous environments typical of pulverized coal combustors. With the model, the extent to which fragments might extinguish and hence, contributes to unburned carbon in ash can be predicted.

## TABLE OF CONTENTS

RESEARCH OBJECTIVES.....	i
TECHNICAL PROGRESS DURING THIS QUARTER.....	1
Summary.....	1
Task 3. Char Fragmentation Studies.....	1
Task 4. Fragmentation Modelling.....	3
Char Particle Fragmentation Behavior during Combustion.....	4
Conclusions of this quarter's work.....	8
PLANS FOR NEXT QUARTER.....	9
REFERENCES.....	10
COMMENT FROM THE PI.....	11
APPENDIX.....	11

## TECHNICAL PROGRESS DURING THIS QUARTER

### SUMMARY

The information reported is for the period October 1 to December 31, 1994. During this quarter, activities were undertaken in Tasks 3 and 4 of the research project. Mass loss measurements were made for a 58% porosity char burning in a flow reactor environment containing 12 mole-% oxygen. Temperatures along the reactor centerline ranged from 1550 K near the reactor inlet to 1450 K at a height of 25.4 cm above the inlet (at a particle residence time of approximately 117 ms). The size distributions of the char fed to the reactor and of the char extracted from the reactor at the 25.4 cm level were determined using the Coulter Multisizer. Also during the quarter, the particle population model was modified to allow for burning at rates at fixed fractions of the diffusion-limited rates. The parameter  $\chi$ , defined as the ratio of the actual overall particle burning rate to the diffusion-limited burning rate, was employed.

Parameters in the particle population model were adjusted to provide agreement between predicted and measured overall particle mass loss rates and size distributions at the 25.4 cm height in the flow reactor. When it was assumed that particle fragmentation was insignificant, the predicted particle size distribution did not match the one measured when  $\chi$  was adjusted to obtain agreement between the measured and calculated  $m/m_0$ . When it was assumed that fragmentation was of the attritive or breakage types, no values of  $\chi$  and  $k$  (the fragmentation rate coefficient) could be determined that yielded results that agreed with the measurements. Agreement could be obtained when percolative-type fragmentation was assumed, however. Model parameters indicate that on average, particles were burning at 46% of their diffusion-limited rates (*i.e.*,  $\chi = 0.46$ ). The fragmentation rate coefficient  $k$ , was found to be  $0.06 \mu\text{m}^{-1}\cdot\text{s}^{-1}$ , which corresponds to roughly 45% of the number of particles having initial diameters of 90  $\mu\text{m}$  producing fragments during the 117 ms of time spent in the flow reactor.

### TASK 3: CHAR FRAGMENTATION STUDIES

Particles in the 90 to 106  $\mu\text{m}$  size range of a synthetic char having a porosity of 58% and an apparent density of 0.62 g/cc were injected into a flow reactor environment having 12 mole-% oxygen. Temperatures along the reactor centerline ranged from 1550 K near the reactor inlet to 1450 K at the 25.4 cm height in the reactor where particles were extracted. Particle residence times to this height were about 117 ms.

The ratio  $m/m_0$  was determined from measurements of the weight of char fed to the flow reactor and the weight of char that was collected. Based on previous work (Mitchell, *et al*, 1992), this method is accurate to better than 10%. The measurements indicate that 25% of the initial char mass remained (*i.e.*,  $m/m_0 = 0.25$ ) at the 117 ms residence time in the flow reactor.

Three samples of the char fed to the reactor and three samples of the char collected at the 25.4 cm sampling height were run through the Coulter Multisizer to determine the size distributions of the unburned and partially burned chars. The cumulative number distributions measured for the three unburned char samples were in excellent agreement as were the cumulative number distributions measured for the three partially reacted char samples. In the figures discussed below, only the averages of the distributions are presented.

Figure 1 shows the cumulative number distributions that were measured for the unburned and burned chars. Note that the unburned char had a large number of particles below 10  $\mu\text{m}$  (about 70% of the total number of particles sampled), and relatively few particles between 20 and 60  $\mu\text{m}$ . The partially reacted char had a significant reduction in the number of small particles and a significant increase in the number of particles in the 20 to 60  $\mu\text{m}$  size range. Clearly, some of the smaller particles in the injected char were completely burned and some of the larger particles were reduced in size via oxidation and fragmentation.

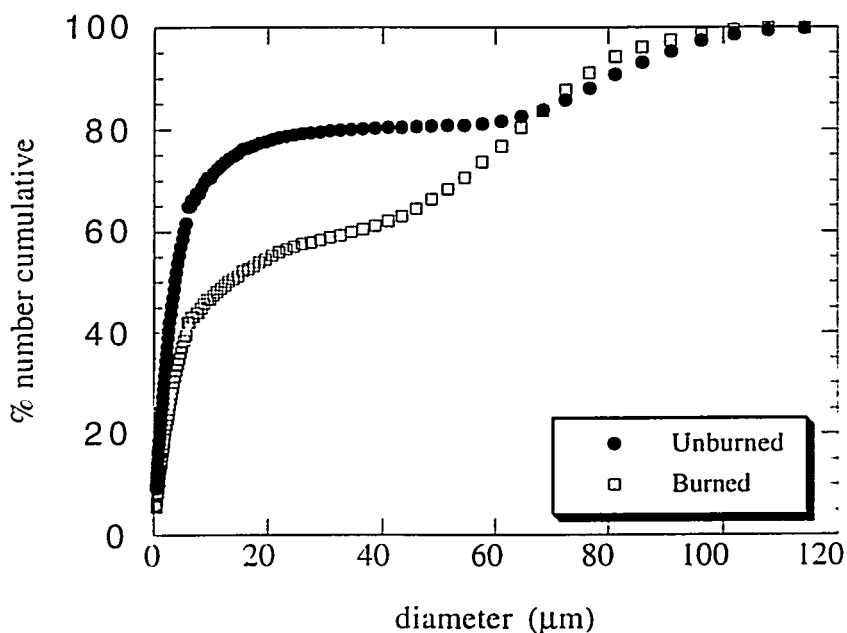


Figure 1. Measured cumulative number distributions of unburned and burned ( $m/m_0 = 0.25$ ) chars.

Figure 2 shows that on a mass basis, the mean particle size of the unburned char is about 90  $\mu\text{m}$  and that little of the mass is comprised of particles having diameters less than 55  $\mu\text{m}$ . The figure also shows that the mean particle size was reduced to about 75  $\mu\text{m}$  as a result of burning. A significant portion of the mass of the partially burned char is in the size range 40 to 60  $\mu\text{m}$ , a range that initially contained relatively little of the total mass.

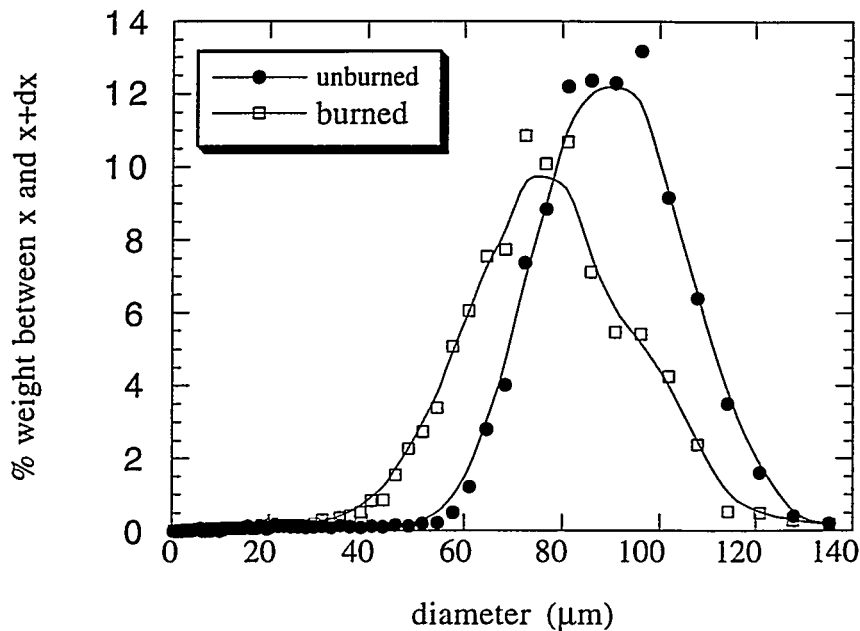


Figure 2. Measured mass distributions of unburned and burned ( $m/m_0 = 0.25$ ) chars.

## TASK 4: FRAGMENTATION MODELLING

### Modification of the Particle Population Model

The particle population model that describes the changes in the numbers of particles of various sizes during combustion and inherent fragmentation has been presented in previous quarterly reports (for example, see Diaz and Mitchell, 1994). The model is represented by a set of differential equations of the following form:

$$\frac{dN_i}{dt} = -S_i N_i + \left( \sum_{j=1}^i b_{ij} S_j N_j \right) - C_i N_i + C_{i-1} N_{i-1} \quad i = 1, n \quad (C_0 = N_0 \equiv 0) \quad (1)$$

where  $N_i$  represents the number of particles within any discrete size class  $i$ . The parameters  $S_i$  and  $C_i$  are the fragmentation and burning rate constants, respectively, and  $b_{ij}$  are the

elements of the fragmentation progeny matrix, which depend upon the type of fragmentation (attrition, breakage, or percolation) assumed. The fragmentation rate constant gives the fraction of the total number of particles of size  $x_i$  that are fragmenting per unit time and is expressed as:

$$S_i = kx_i^\alpha \quad k > 0 \quad \alpha \geq 0 \quad (2)$$

where the frequency of fragmentation events per unit particle size is given by the fragmentation rate coefficient  $k$ , and the relative tendency for a particle of size  $x_i$  to fragment is given by the particle sensitivity parameter  $\alpha$ .

The burning rate constant gives the fractional rate of change of the total number of particles of size  $x_i$  that are reduced in size as a consequence of burning and leave the size class. The constant was modified to allow for burning at fixed fractions of the diffusion-limited rates, and is given as follows:

$$C_i = \frac{4 M_C D_{O_2} P_g}{\rho_p R T_g v_o} \frac{\chi}{x_i^{2\gamma-1}} \quad (3)$$

where  $\chi$  is the ratio of the actual particle burning rate to the diffusion-limited burning rate;  $M_C$ , the molecular weight of carbon;  $D_{O_2}$ , the bulk diffusion coefficient of oxygen;  $P_g$ , the oxygen partial pressure in the ambient gas;  $\rho_p$ , the particle apparent density;  $R$ , the gas constant,  $T_g$ , the gas temperature; and  $v_o$ , the stoichiometric oxygen coefficient (equal to one-half for CO formation). The use of  $\chi$  to affect non-diffusion-limited burning has been employed previously, as indicated in the review by Smith (1982). This simple treatment to account for the effects of pore diffusion and the intrinsic chemical reactivity of the particle material was adopted because at the present time, reaction rate parameters for the synthetic chars have not been determined and we have not yet determined flow reactor environments that render diffusion-limited burning. Presently, the model assumes that particles burn as shrinking spheres at constant density.

## CHAR PARTICLE FRAGMENTATION BEHAVIOR DURING COMBUSTION

The particle population model was used to characterize the type of fragmentation occurring while the char particles burned in the flow reactor. In the calculations, one hundred logarithmically-spaced size classes were used with  $x_i/x_{i+1} = 1.0585$ . For the largest size class of particles,  $x_l = 139 \mu\text{m}$  and for the smallest size class,  $x_n = 0.5 \mu\text{m}$ . The set of 100

differential equations describing the changes in the numbers of particles in each size class were solved using LSODE, a Runge-Kutta variable-step, ODE solver developed by Radhakrishnan and Hindmarsh (1983). The number distribution of the unburned char was used as the initial number distribution in the calculations and values of  $\chi$  and  $k$  were adjusted to get agreement between the measured and predicted  $m/m_0$  and particle number distributions at the 117 ms residence time. The fragmentation sensitivity parameter  $\alpha$  was taken as 1.0, based on the investigations of Dunn-Rankin (1988) and Austin *et al.* (1984).

When it was assumed that fragmentation did not occur ( $k$  set to zero), the predicted number distribution did not match the one measured when  $\chi$  was adjusted to get agreement between measured and calculated  $m/m_0$ . When it was assumed that fragmentation was of the attritive or breakage types, no values of  $\chi$  and  $k$  could be determined that yielded results that agreed with the measurements. Figures 3 and 4 show predicted cumulative distributions when breakage-type fragmentation is assumed. Calculations are shown for values of  $k$  equal to 0, 0.04, 0.8 and  $2.7 \mu\text{m}^{-1}\text{s}^{-1}$ . For each of the predicted curves,  $m/m_0$  equals 0.25, in agreement with the measured value at the 25.4 cm height in the reactor. The curve for  $k = 0$  is the no-fragmentation case; increasing values of  $k$  give increasing frequency of breakage-type fragmentation events.

Figure 3 shows comparisons between the cumulative size distributions when expressed on a mass basis. The distribution calculated when  $k = 0$  coincides best with the measured size distribution. However, when the distribution is expressed on a number basis, the agreement is poor. This is illustrated in Fig. 4, which reveals that none of the predicted cumulative number distributions agree with the measured distribution when breakage-type fragmentation is assumed. For  $k = 0.04 \mu\text{m}^{-1}\text{s}^{-1}$ , agreement is adequate for large particle sizes, but for sizes less than  $70 \mu\text{m}$ , agreement is inadequate. Larger values of  $k$  result in too much breakage of the large particles. No combinations of  $k$  and  $\chi$  could be determined that yielded a number cumulative distribution that had the characteristic shape of the measured distribution.

For the cases shown in Figs. 3 and 4, breakage was assumed to result in the formation of two fragments that fall into the next lower size class from the fragmenting particle. Variations in the fragmentation size sensitivity parameter  $\alpha$  did not lead to distributions significantly different from those shown in the figure nor did assuming that breakage resulted in two to three fragments that fall into the next two lower size classes from the fragmenting particles. We conclude that breakage is not the type of fragmentation that is occurring as the particles are burning in the flow reactor.

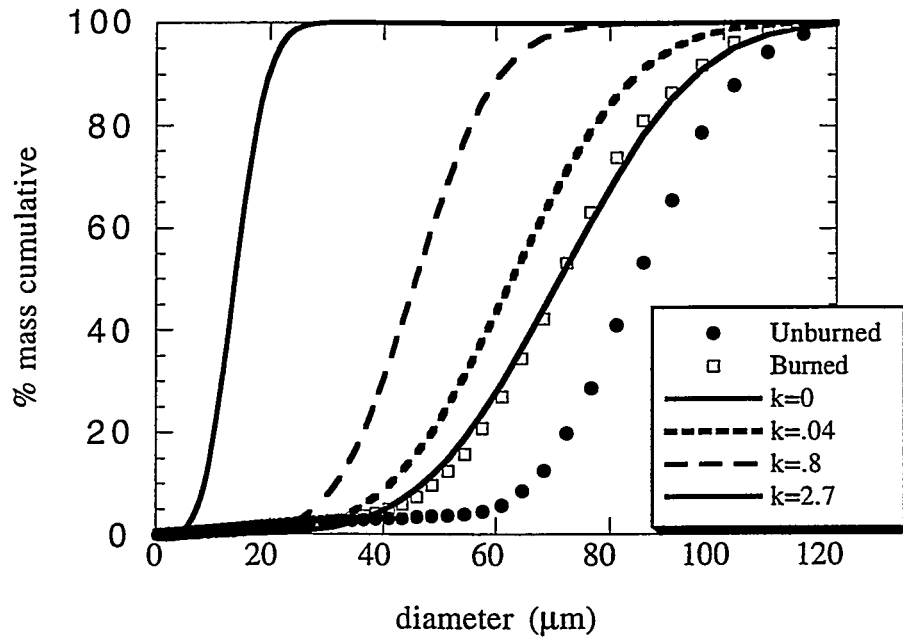


Figure 3. Calculated and measured cumulative mass distributions of unburned and burned ( $m/m_0 = 0.25$ ) chars. Breakage-type fragmentation is assumed. The fragmentation rate coefficient  $k$  has units  $\mu\text{m}^{-1}\cdot\text{s}^{-1}$ .

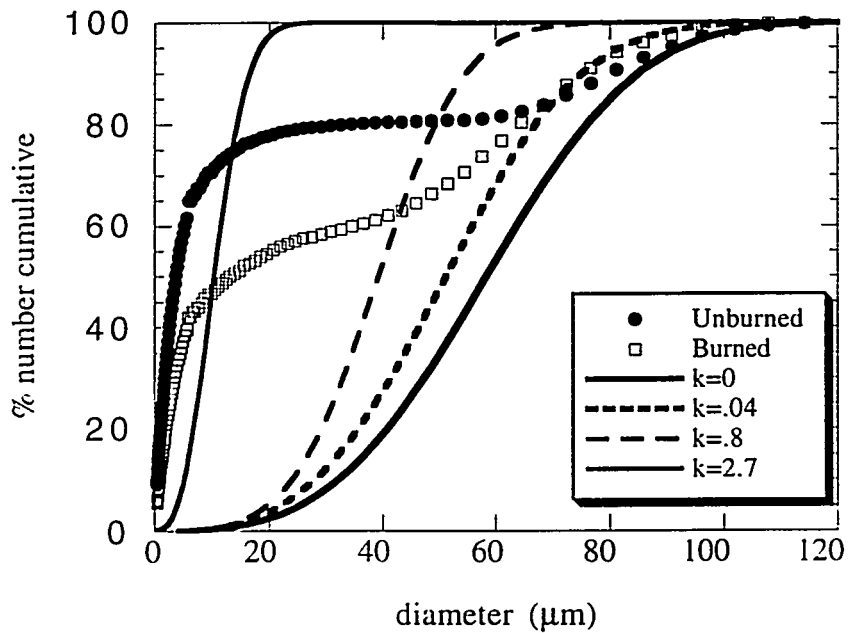


Figure 4. Calculated and measured cumulative number distributions of unburned and burned ( $m/m_0 = 0.25$ ) chars. Breakage-type fragmentation is assumed. The fragmentation rate coefficient  $k$  has units  $\mu\text{m}^{-1}\cdot\text{s}^{-1}$ .

Figures 5 and 6 show the agreement that can be obtained assuming percolative-type fragmentation. The calculated cumulative mass and number distributions are in good agreement with the measured distributions. The model does slightly overpredict the number of particles having diameters below 20  $\mu\text{m}$  (see Fig 6), but for sizes greater than 20  $\mu\text{m}$ , the numbers of particles in the various size bins are adequately predicted. Figure 7 shows that the predicted weight distribution is also in good agreement with the measured distribution. The predicted mean size is 78  $\mu\text{m}$ , by weight, in agreement with measured value of 75  $\mu\text{m}$ . Model parameters indicate that on average, particles were burning at 46% of their diffusion-limited rates (*i.e.*,  $\chi = 0.46$ ). The fragmentation rate coefficient  $k$ , was found to be  $0.06 \mu\text{m}^{-1}\text{s}^{-1}$ , which corresponds to roughly 45% of the particles initially having diameters of 90  $\mu\text{m}$  producing fragments during the 117 ms of time spent in the flow reactor. Some of these fragments are relatively large, having sizes that place them into bins in the 30 to 70  $\mu\text{m}$  size range, but most of them are small, having sizes less than 20  $\mu\text{m}$ .

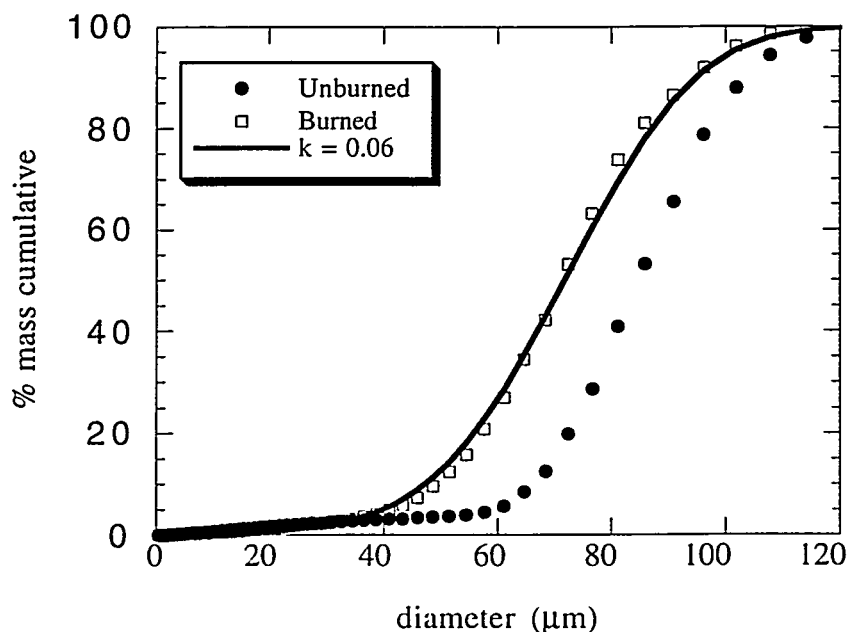


Figure 5. Calculated and measured cumulative mass distributions of unburned and burned ( $m/m_0 = 0.25$ ) chars. Percolative-type fragmentation is assumed. The fragmentation rate coefficient  $k$  has units  $\mu\text{m}^{-1}\text{s}^{-1}$ .

The calculations show that fragmentation is responsible for maintaining a significant number of particles in the smaller size ranges. If there were no fragmentation, all particles in the unburned char having diameters less than 70  $\mu\text{m}$  would have reached burnout before the

117 ms residence time in the reactor if they burned at rates near 46% of their diffusion-limited rates throughout their burn-times. Of the particles in the unburned char having diameters greater than 70  $\mu\text{m}$ , less than 5% of them would have burned to have diameters less than 20  $\mu\text{m}$ , and not as many as 50% as the measurement indicates. The increased number is due to fragmentation.

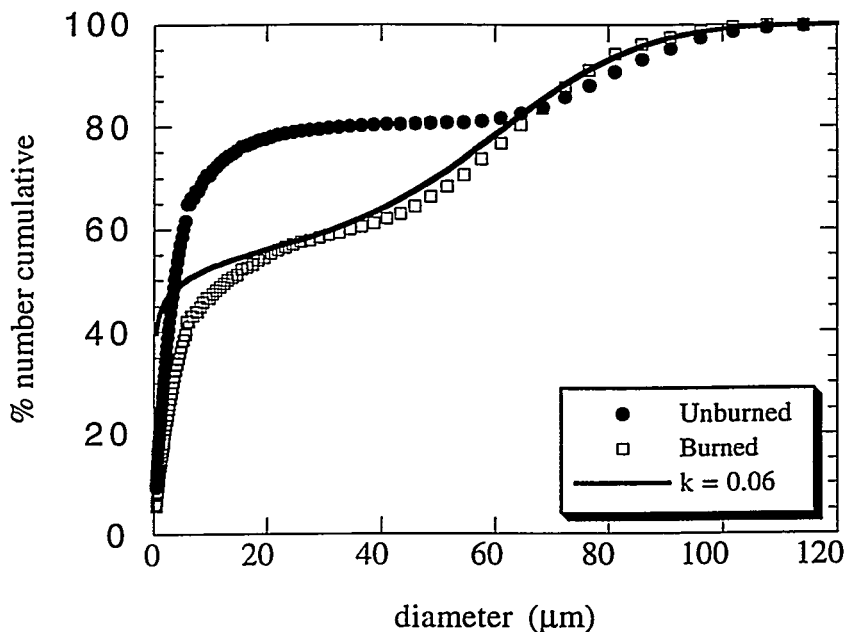


Figure 6. Calculated and measured cumulative number distributions of unburned and burned ( $m/m_0 = 0.25$ ) chars. Percolative-type fragmentation is assumed. The fragmentation rate coefficient  $k$  has units  $\mu\text{m}^{-1}\cdot\text{s}^{-1}$ .

## CONCLUSIONS OF THIS QUARTER'S WORK

During the char oxidation phase of pulverized coal combustion, particles fragment. The fragmentation behavior can be characterized as being percolative, where fragmenting particles produce fragments of all sizes. With the 58% porosity char used in the experiments, fragmentation events were quite frequent, with about 45% of the particles initially having a diameter of 90  $\mu\text{m}$  producing fragments during the 117 ms residence time spent burning in the flow reactor.

Since overall particle burning rates depend upon particle size, it is apparent that accurate prediction of mass loss during the char oxidation phase of coal combustion requires that account is made for char particle fragmentation. The particle population model developed

is limited presently to constant density, diffusion-controlled burning. Before the effects of fragmentation on the extent of mass loss can be examined in greater detail, the model must be modified to allow for variable density burning and for burning limited by the combined effects of pore diffusion and the intrinsic chemical reactivity of the carbonaceous particle material.

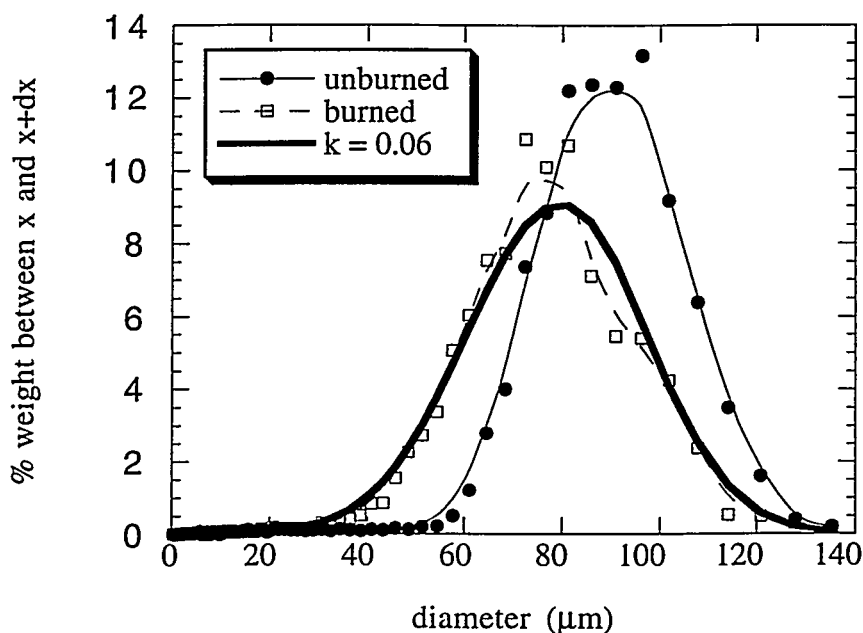


Figure 7. Calculated and measured mass distributions of unburned and burned ( $m/m_0 = 0.25$ ) chars. Percolative-type fragmentation is assumed. The fragmentation rate coefficient  $k$  has units  $\mu\text{m}^{-1}\cdot\text{s}^{-1}$ .

### PLANS FOR NEXT QUARTER

During the next quarter, we will continue to obtain combustion data on synthetic chars burning in selected flow reactor environments. The data will be used to characterize the type of fragmentation and to determine the fragmentation rate. Experiments will be aimed at determining how the fragmentation rate coefficient varies with char porosity. It is expected that the higher the porosity, the greater the tendency for particles to fragment and hence, the higher the fragmentation rate coefficient. Specific plans for next quarter are listed below.

- Generalize the form of the burning rate constant  $C_i$  in the particle population model beyond the restriction of shrinking-sphere burning. Allowance will be made for mixed-

mode burning where both the apparent density and size of the particle decrease with mass loss.

- Produce additional synthetic chars differing in porosity and mineral content.
- Obtain additional mass loss and size distribution data on partially reacted chars. Use the data to determine burning and fragmentation parameters.

## REFERENCES

Austin, L. G., Klimpel, R. R., and Luckie, P. T., *Process Engineering of Size Reduction: Ball Milling*, Society of Mining Engineers, New York, 1984.

Diaz, R. and Mitchell, R.E., "Char Particle Fragmentation and its Effect on Unburned Carbon During Pulverized Coal Combustion," DOE/PETC Quarterly Progress Report for January to March, 1994, DOE/PC/92528-6 (1994)

Dunn-Rankin, D., *Combustion Science & Technology*, 58:297 (1988).

Smith, I. W., "The Combustion Rates of Coal Chars: A Review", *Nineteenth Symposium (International) on Combustion*/The Combustion Institute, 1045 (1982).

Mitchell, R.E., Hurt, R.H., and Hardesty, D.R. , "Compilation of Sandia Coal Char Combustion Data and Kinetic Analyses: Milestone Report," Sandia National Laboratories, SAND92-8208 (1992).

Radhakrishnan, K. and Hindmarsh, A.C. , "Description and Use of LSODE, the Livermore Solver for Ordinary Differential Equations", Lawrence Livermore National Laboratories, UCRL-ID-113855 (1993)

## PRESENTATION

A paper based on the work reported in this quarterly report is being presented at the Joint Central States/Western States/Mexican National/American Flame Research Committee Meeting that is being held April 23-26, 1995 in San Antonio, Texas. The paper is entitled

"The Effect of Porosity on Char Particle Fragmentation during Pulverized Coal Combustion."  
The six-page paper is included below as Appendix A.

### **COMMENT FROM THE PI**

During this quarter, Ruben Diaz, the graduate student who has been working on this project since its inception, terminated his Ph. D. program. Another graduate student was assigned to the project. The transition caused a temporary disruption in the steady progress that was being made and delayed the preparation of this quarter report.

### **APPENDIX**

The following paper is being presented at the the Joint Central States/Western States/Mexican National/American Flame Research Committee Meeting that is being held April 23-26, 1995 in San Antonio, Texas.

# The Effect of Porosity on Char Particle Fragmentation during Pulverized Coal Combustion

REGINALD E. MITCHELL, RUBEN DIAZ, and GAYLE V. RAMDEEN

*High Temperature Gasdynamics Laboratory, Mechanical Engineering Department, Stanford University, Stanford, CA*

Synthetic char particles with controlled macroporosity are used to study char fragmentation behavior during pulverized coal combustion. The chars are burned in an atmospheric laminar flow reactor that permits the control of gas temperature and composition. Char particles are extracted from the reactor at selected residence times and characterized for extent of mass loss, apparent density, porosity, and particle size distribution. Differences in mass loss rates are attributed to fragmentation events, the extent of which are determined from the measured size distributions.

A particle population balance model is used to describe changes in the particle size distribution with time as a result of burning and fragmentation. The model can allow for attritive-type behavior (in which only fines are produced), breakage-type behavior (in which particles break into two or three smaller particles), and percolative-type behavior (in which particles fragment into a distribution of smaller size particles). Model parameters are adjusted to provide time-resolved agreement with measured overall mass loss rates and particle number distributions. The model is used to characterize the type of fragmentation that occurs during char oxidation and to quantify the rate of fragmentation events.

## INTRODUCTION

A significant number of char particles that are formed during the devolatilization phase of pulverized coal combustion have relatively large void volumes within them. Large voids at the outer surfaces of particles allow oxygen to consume the inner particle material. As a consequence, particles may fragment as interior surfaces are consumed via chemical reaction. Char fragments burn at rates governed by their individual sizes and not at rates controlled by the sizes of their parent particles. Consequently, overall mass loss rates depend upon the extent of fragmentation.

Some of the fragments that are formed during char oxidation have shapes that are quite irregular and may have high external surface-to-volume ratios. The radiative and convective energy losses from such particles can exceed the energy generated within them via reaction causing some particles to extinguish. It is likely that char fragmentation influences the extent of unburned carbon found in the ash during pulverized coal combustion. This paper reports on preliminary work aimed at characterizing the impact of fragmentation on unburned carbon during pulverized coal combustion. The effect of porosity on char particle fragmentation is investigated by

burning chars differing in porosity and examining the extent of fragmentation as evidenced by differences in particle size distributions.

Figure 1 illustrates the three types of fragmentation behavior considered: attrition, breakage, and percolation. During attritive fragmentation, numerous small fragments (fines) abrade from the periphery of parent particles as particles collide with one another and/or impact surfaces within their surroundings. Throughout the process, the overall sizes of the parent particles diminish only slightly. During breakage fragmentation, only a few fragments are produced and these are relatively large, having sizes not much smaller than their parent particles.

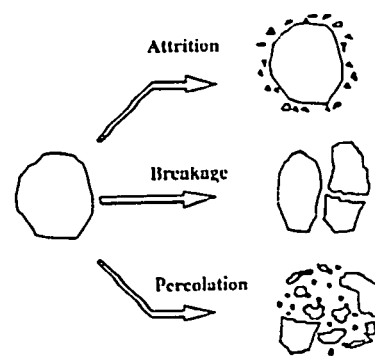


Figure 1. Types of fragmentation behavior

Percolative fragmentation refers to the transition from a connected solid network to a completely fragmented state. Whereas attrition produces fine fragments and breakage produces relatively large fragments, percolative fragmentation produces fragments having a range of sizes, from the sizes of the parent particles to the sizes of the fine particles.

## EXPERIMENTAL APPROACH

In experiments designed to characterize the extent of char fragmentation during combustion, synthetic chars with controlled porosities are used in order to eliminate the complications associated with the heterogeneity of real coal chars. The synthetic char particles have morphologies similar to those of the char particles formed during coal devolatilization. The chars vary in the nature of their porosity and pore size distribution. The chars are produced from the polymerization of furfuryl alcohol with p-toluenesulfonic acid in water, following the procedures developed by Senior [1] and Senior and Flagan [2]. Particle pore size distributions are altered by varying the relative amounts of micropore- and macropore-formers added during the synthesis procedure. Carbon black particles (nominally 20 nm in diameter) are used as micropore-formers. Carbon black increases the microporosity by causing the carbonized furfuryl alcohol matrix to crack around the locations of the carbon black inclusions [3].

The spores of lycopodium plants are used as macropore-formers. Akan-Etuk and Niksa [4] found that the addition of lycopodium plant spores produce macropores of a uniform size (nominally 20  $\mu\text{m}$  in diameter) when they vaporize during the thermal curing step of the synthesis procedure. The chars produced are ground and size classified into the size ranges 76-89  $\mu\text{m}$ , 90-106  $\mu\text{m}$ , and 106-125  $\mu\text{m}$ . Helium pycnometry is used to determine the true density of the carbonaceous material and mercury intrusion porosimetry combined with a tap density procedure [5] is used to determine apparent particle densities.

Chars of selected porosity and size are burned in an atmospheric, laminar, entrained flow reactor that permits the control of gas temperature and composition. The flow reactor is similar in

design to that used in the coal char oxidation studies by Mitchell *et al.* [5]. The oxygen content of the hot reactor gases can be varied from trace amounts up to about 21% (by volume) and the gas temperature can be varied from about 1250 K to almost 2100 K.

Particles are injected along the reactor centerline and extracted from the reactor at selected residence times using a helium-quench solids sampling probe. The partially reacted char particles are characterized for apparent densities, porosities, and pore size and particle size distributions. The size distributions are measured with a Coulter Multisizer, employing an orifice tube with an aperture diameter sufficient to measure particle diameters in the range 5.6 to 168  $\mu\text{m}$ .

## THEORETICAL APPROACH

In our description of the particle size distribution, a number of discrete size intervals (size bins) are used. Bin  $i$  is characterized by its upper and lower size cutoffs,  $x_i$  and  $x_{i+1}$ , respectively. Bin 1 contains the largest size particles in the distribution (diameters in the range  $x_1$  to  $x_2$ ) and bin  $n$ , the smallest size particles (diameters in the range  $x_n$  to 0). The upper and lower size cutoffs of each size interval vary by a constant factor  $\gamma$ , which is defined as:

$$\gamma = \frac{x_i}{x_{i+1}} \quad (1)$$

This treatment yields uniformly spaced size intervals in the log-domain ( $\ln x_i - \ln x_{i+1} = \ln \gamma = \text{constant}$ ), and is effective in accurately resolving the size distribution in the small-size range where particle number densities can be quite large relative to the number densities in the large-size range.

A particle population balance model is used to describe changes in the particle size distribution with time as a result of char oxidation and fragmentation. Our approach is similar to that of Dunn-Rankin [6], who modified the model developed by Austin *et al.* [7] for simulating the grinding of particles using a ball mill. The model is represented by a differential equation of the following form for each bin  $i$ :

$$\frac{dN_i}{dt} = -S_i N_i + \left( \sum_{j=1}^i b_{ij} S_j N_j \right) - C_i N_i + C_{i-1} N_{i-1} \quad (2)$$

where  $N_i$  represents the number of particles within bin  $i$ .  $S_i$  and  $C_i$  are the fragmentation and burning rate constants, respectively, and  $b_{ij}$  are elements of the fragmentation progeny matrix, which specify the number of fragments that enter bin  $i$  per particle that fragments in bin  $j$ .

The fragmentation rate constant gives the fraction of particles of size  $x_i$  that are fragmenting per unit time and is expressed as:

$$S_i = kx_i^\alpha \quad (3)$$

where the frequency of fragmentation events per unit particle size is given by the fragmentation rate coefficient  $k$ , and the relative tendency for a particle of size  $x_i$  to fragment is given by the particle sensitivity parameter  $\alpha$ . Based on the investigations of Dunn-Rankin [6] and Austin *et al.* [7],  $\alpha$  is taken as unity.

The burning rate constant describes the mass loss rates of particles of size  $x_i$  and is given as follows:

$$C_i = \frac{4 M_C D_{O_2} P_g}{\rho_p R T_g v_o} \frac{\chi}{x_i^2 (\gamma - 1)} \quad (4)$$

where  $\chi$  is the ratio of the actual particle burning rate to the diffusion-limited burning rate;  $M_C$ , the molecular weight of carbon;  $D_{O_2}$ , the bulk diffusion coefficient of oxygen;  $P_g$ , the oxygen partial pressure in the ambient gas;  $\rho_p$ , the particle apparent density;  $R$ , the gas constant,  $T_g$ , the gas temperature; and  $v_o$ , the stoichiometric oxygen coefficient (equal to one-half for CO formation). Presently, the model assumes that particles burn as shrinking spheres at constant density.

The distribution of fragments is specified by the elements of the fragmentation progeny matrix,  $b_{ij}$ . Particles fragmenting in bin  $j$  can produce fragments only in bin  $i$  where  $i \geq j$ , therefore,  $b_{ij} = 0$  for  $i < j$ . Volume conservation places a constraint on  $b_{ij}$ . Conservation of volume (and also mass if all particles are assumed to have the same constant apparent density) requires that

$$x_j^3 = \sum_{i=1}^n b_{ij} x_i^3 \quad (5)$$

where  $x_j$  is the size of the fragmenting particle and  $x_i$ 's are the sizes of the resultant spherical fragments that fall into the allowable size bins. Allowable size bins include the bin containing the fragmenting particles (bin  $j$ ) and the bins containing the smaller size classes of particles (bin  $j+1$  to bin  $n$ ).

Depending upon the type of fragmentation, some of the  $b_{ij}$  elements may be zero for  $i \geq j$ . For example with breakage, fragments may be produced in only the next two lower size classes, and  $b_{ij}$  would be set to zero for all  $i$  except  $i = j+1$  and  $i = j+2$ . With attrition, fragments could fall into the size bins associated with the smallest size classes (say, bin  $m$  to bin  $n$ , where  $m = n-2$  for the smallest three size classes) as well as into size bin  $j+1$  (as those particles having sizes near the lower cutoff of the  $j$ -th size class are reduced in size, moving them into the next lower size class). In this case,  $b_{ij}$  would be set to zero for  $i = j+2$  to  $i = m-1$ . With percolation, fragments could fall into all size bins, bin  $j$  to bin  $n$ . None of the elements of the percolation progeny matrix for  $i \geq j$  would be set to zero.

Non-zero elements of the fragmentation progeny matrix also depend on the type of fragmentation occurring. These are discussed below for attrition (where many submicron fragments are produced), breakage (where two or three fragments of more or less equal sizes are produced), and percolation (where a family of fragments of all sizes smaller than the fragmenting particle are produced).

### Attrition

Attrition behavior is modelled by assuming that each particle undergoing attrition in bin  $j$  loses a small fraction  $f$  (taken as 0.1%) of its mass from its periphery during a single fragmentation event. One large fragment is produced (actually, the parent particle) that remains in bin  $j$  (or possibly enters bin  $j+1$  if the particle had a diameter near the lower size cutoff of bin  $j$ ) and numerous small fragments are produced that fall into bins  $m_j$  to  $n$ . The subscript  $j$  on  $m_j$  indicates that the size of the largest attrited fragments depends on the size of the attriting particle. For attrition, elements of the progeny matrix are evaluated as follows:

$$b_{ij} = \begin{cases} 0 & j+2 \leq i \leq m_j - 1 \\ \frac{f\gamma^3}{n - m_j + 1} & m_j \leq i \leq n \\ \frac{(1-f)\gamma^3 - 1}{\gamma^3 - 1} & i = j \\ \frac{f\gamma^3}{\gamma^3 - 1} & i = j+1 \\ 0 & i = n \text{ or } i < j \end{cases} \quad (6)$$

Presently, we assume that attrited particles fall only into the size bin containing the smallest particle sizes. Accordingly,  $m_j$  is set equal to  $n$ , with  $x_n = 0.5 \mu\text{m}$ .

### Breakage

For particles undergoing breakage, only a few fragments are produced, and these have sizes close to the sizes of the fragmenting particles. For breakage in size bin  $j$ , fragments may fall into size bins  $j$  to  $j+l$ , where  $l$  is say, two. For breakage, progeny matrix elements are expressed as:

$$b_{ij} = \begin{cases} 0 & i < j \\ \frac{\gamma^{\beta(i-j)}}{\sum_{k=1}^{l+1} \gamma^{k(\beta-3)}} & j \leq i \leq j+l \\ 0 & i > j+l \end{cases} \quad (7)$$

Presently, we assume breakage into two fragments that fall into the next lower size class from the fragmenting particle. For this situation the elements of the progeny matrix are given by:

$$b_{ij} = \begin{cases} 0 & i \leq j \\ \gamma^3 & i = j+1 \\ 0 & i > j+1 \end{cases} \quad (8)$$

### Percolation

Results from the percolation model of char oxidation used by Kerstein and Edwards [8]

indicate that at high carbon conversions the fragment number distribution varies linearly with mass on a log-log plot. Their results indicate that a single particle ultimately yields a family of fragments such that logarithmically spaced size bins each contain an equal mass fraction of the original particle. This is additional justification for our using logarithmically spaced size bins. Assuming that the apparent densities of all particles and their fragments are the same, equal mass fractions of the original particle being distributed to each size bin is analogous to equal volumes of the fragmenting particles being distributed to each size bin. Employing this result, the elements of the progeny matrix for percolation can be expressed as:

$$b_{ij} = \begin{cases} \frac{\gamma^{3(i-j)}}{n - j + 1} & i \geq j \\ 0 & \text{otherwise} \end{cases} \quad (9)$$

The key adjustable parameters in the particle population balance model are  $\chi$ , the ratio of the actual particle burning rate to the diffusion-limited particle burning rate, and  $k$ , the fragmentation rate coefficient. These are adjusted to provide time-resolved agreement between measured and calculated overall mass loss and particle number distributions.

## RESULTS AND DISCUSSION

Figure 2 shows synthetic char particles in the 90 to 106  $\mu\text{m}$  size range having porosities of 16% and 55%. For the 16% porosity char, only carbon black was added during the synthesis procedure. Hence, these particles have no large void volumes within them. Mercury porosimetry indicates that the largest intraparticle pores for the 16% porosity chars are nominally 0.05  $\mu\text{m}$ . It is expected that these char particles will fragment the least when burned.

The extent of fragmentation associated with the particle feeding and collection systems was assessed in cold-flow experiments. Results indicated that the particle feeder and transfer line caused insignificant fragmentation and that the particle collection system caused attritive-type fragmentation. The char collected on the filter paper

had an increased number of particles with sizes less than 20  $\mu\text{m}$ , however, the weight distribution of these particles was essentially the same as the weight distribution of the particles initially placed in the feeder. Predictions using the population balance model with  $\chi = 0$  (no burning) indicate that for flow through the sampling probe and filter housing,  $k = 6.5 \times 10^{-5} \mu\text{m}^{-1} \text{s}^{-1}$ . For this value of  $k$ , almost 0.1% of the particles having diameters of nominally 100  $\mu\text{m}$  produced fragments.



Figure 2. Micrographs of synthetic chars having porosities of 16% (top) and 55% (bottom).

Particles in the 90 to 106  $\mu\text{m}$  size range of a char having a porosity of 58% were injected into a flow reactor environment having 12 mole-% oxygen. Temperatures along the reactor centerline ranged from 1550 K near the reactor inlet to 1450 K at the 25.4 cm height in the reactor where particles were extracted. Particle residence times to this height were about 117 ms.

Figure 3 shows the cumulative number distributions that were measured (data points) for the unburned and burned chars. Note that the

unburned char had a large number of particles below 10  $\mu\text{m}$  (about 70% of the total number of particles sampled), and relatively few particles between 20 and 60  $\mu\text{m}$ . The partially reacted char had a significant reduction in the number of small particles and a significant increase in the number of particles in the 20 to 60  $\mu\text{m}$  size range. Clearly, some of the smaller particles in the injected char were completely burned and some of the larger particles were reduced in size via oxidation and fragmentation.

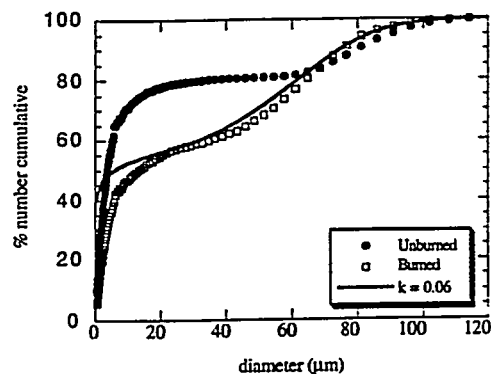


Figure 3. Measured and predicted cumulative number distributions of unburned and burned ( $m/m_0 = 0.25$ ) chars.

Figure 4 shows that on a mass basis, the mean particle size of the unburned char is about 90  $\mu\text{m}$  and that little of the mass is comprised of particles having diameters less than 55  $\mu\text{m}$ . The figure also shows that the mean particle size was reduced to about 75  $\mu\text{m}$  as a result of burning. Weight loss measurements indicate that 25% of the initial char mass remained (*i.e.*,  $m/m_0 = 0.25$ ) at the 117 ms residence time in the flow reactor.

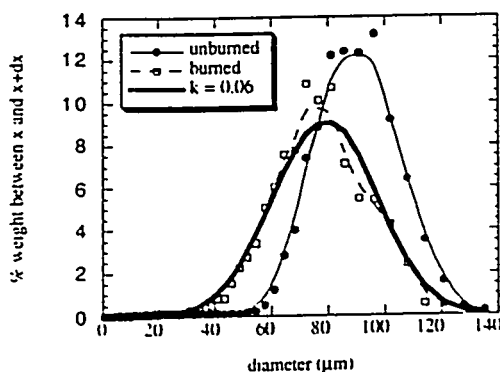


Figure 4. Measured and predicted mass distributions of unburned and burned ( $m/m_0 = 0.25$ ) chars.

The particle population model was used to characterize the fragmentation behavior of the char particles as they burned in the flow reactor. The number distribution of the unburned char was used as the initially number distribution in the calculations and values of  $\chi$  and  $k$  were adjusted to get agreement between the measured and predicted  $m/m_0$  and particle number distributions at the 117 ms residence time. When it was assumed that fragmentation did not occur ( $k$  set to zero), the predicted number distribution did not match the one measured when  $\chi$  was adjusted to get agreement between measured and calculated  $m/m_0$ . When it was assumed that fragmentation was of the attritive or breakage types, no values of  $\chi$  and  $k$  could be determined that yielded results that agreed with the measurements.

The heavy solid lines in Figs. 3 and 4 show the agreement that could be obtained assuming percolative-type fragmentation. The calculated cumulative number distribution is in good agreement with the measured distribution except for particles in the smallest size ranges. The predicted weight distribution is also in good agreement with the measured distribution. Model parameters indicate that on average, particles were burning at 46% of their diffusion-limited rates (*i.e.*,  $\chi = 0.46$ ). The fragmentation rate coefficient  $k$ , was found to be  $0.06 \mu\text{m}^{-1}\cdot\text{s}^{-1}$ , which corresponds to roughly 45% of the particles having initial diameters of  $90 \mu\text{m}$  producing fragments during the 117 ms of time spent in the flow reactor.

Experiments are currently underway to determine how  $k$  varies with char porosity. It is expected that the higher the porosity, the greater the tendency for particles to fragment and hence, the higher the fragmentation rate coefficient.

## CONCLUSIONS

During the char oxidation phase of pulverized coal combustion, particles fragment. The fragmentation behavior can be characterized as being percolative, where fragmenting particles produce fragments of all sizes. Since overall particle burning rates depend upon particle size, it is apparent that accurate prediction of mass loss during the char oxidation phase of coal combustion

requires that account is made for char particle fragmentation.

The particle population model developed is limited presently to constant density, diffusion-controlled burning. Before the effects of fragmentation on the extent of mass loss can be examined in greater detail, the model must be modified to allow for variable density burning and for burning limited by the combined effects of pore diffusion and the intrinsic chemical reactivity of the carbonaceous particle material.

*This work is supported by the U. S. D. O. E. through the Pittsburgh Energy Technology Center.*

## REFERENCES

1. Senior, C.L., PhD Thesis, "Submicron Aerosol Formation During Combustion Of Pulverized Coal," California Institute of Technology, 1984.
2. Senior, C.L. and Flagan, R.C., *Twentieth Symposium (Intl.) on Combustion*, The Combustion Institute, Pittsburgh, 1984, p. 921.
3. Levensis, Y.A. and Flagan, R.C., *Carbon*, 27:265 (1989).
4. Akan-Etuk, A. and Niksa, S., *Energy and Fuels*, 5:614 (1991).
5. Mitchell, R. E., Hurt, R. H., Baxter, L. L., and Hardesty, D. R., "Compilation of Sandia Coal Char Combustion Data and Kinetic Analyses: Milestone Report", Sandia National Laboratories, September 1991.
6. Dunn-Rankin, D., *Combustion Science & Technology*, 58:297 (1988).
7. Austin, L. G., Klimpel, R. R., and Luckie, P. T., *Process Engineering of Size Reduction: Ball Milling*, Society of Mining Engineers, New York, 1984.
8. Kerstein, A. R. and Edwards, B. F., *Chemical and Engineering Science*, 42:1629 (1987).